A THEORETICAL COMPUTER MODEL OF CELLULAR MODIFICATION ASSOCIATED WITH OLFACTORY LEARNING IN THE RAT PIRIFORM CORTEX

G. Gradwohl[a,b*] and Y. Grossman[a]

[a] Department of Physiology, Faculty of Health Sciences, Zlotowsky Center for Neuroscience, Ben-Gurion University of the Negev, Beer-Sheva 84105, Israel. [b] Department of Software Engineering, Negev Academic College of Engineering, Beer-Sheva 84100, Israel.

* Corresponding author: E-mail address: gidig@nace.ac.il

Keywords: Computer simulations, pyramidal piriform neurons, learning, enhanced inhibition, decreased AHP amplitude

Abstract

Learning associated cellular modifications were previously studied experimentally in the rat piriform cortex after operand conditioning. The results showed a 19% reduction in the level of the action potential AHP in trained rats, while the spike trains indicated decreased adaptation during long depolarization. Paradoxically, this reduced AHP amplitude was associated with a level of depression in the EPSP amplitude, which was significantly higher in trained rats than in the control groups, the pseudo-trained and naive rats.

Our goal in the present study is to analyze and explain through computational techniques the effect of increased EPSP depression after learning. We apply three different models to simulate the exact reduction in the AHP amplitude: (1.) *"Conductance change:"* Controlled by decreasing g_{kCa} by 40 %. (2.) *"Moving:"* Shifting the location of the dendritic segment that exhibits active conductances, including AHP conductance, distally from the soma, while decreasing g_{kCa} by only 15%. (3.) "*Shrinkage:"* Decreasing the length of the AHP dendritic segment, while increasing g_{kCa} by 9%. Moving the synaptic input distally from the soma enhances EPSP depression by the AHP conductance. Hence, the learning process could be simulated by a "jump" from the control curve to any other curve, representing decreased AHP amplitude. At the same time, the enhanced EPSP depression requires an additional shift of the EPSP input to more distal locations.

Introduction

We have previously conducted laboratory experiments of cellular modifications, associated with olfactory learning in the rat piriform cortex following operand conditioning [1-5]. Trained rats were trained in a 4-arm maze to discriminate positive cues in pairs of odors. Training continued until rats acquired the rule of learning, typically after learning the first or second pair of odors. Pseudo-trained and naive rats served as controls. Pseudo-trained rats were randomly rewarded, thus preventing them from acquiring any learning skills, while the naive rats were never exposed to the experimental

protocol. The training led to a reduction of the action potential after-hyperpolarization (AHP) in the pyramidal cells in the trained rats, while also decreasing the cells' firing adaptation during depolarizing voltage step. A later study showed that the learning process mainly reduced the slow $I_{AHP,}$ a Ca^{2+}-dependent potassium current that dominates AHP amplitude (Bosh and Barkai, unpublished). EPSPs evoked by neighboring pyramidal cells were increased after training. Intriguingly, inhibition of these EPSPs during maximal AHP conductance, following a short train of action potentials, was more effective after learning than before learning [3].

The goal of the present study is twofold: first to computationally simulate the results, and second to explain why the trained rats' inhibition of EPSP, during maximal AHP conductance, is more effective, despite the reduction in the AHP amplitude. We explore alternative models, defined by changes in size, location, or maximal potassium conductance of the AHP. We suggest that a change in the distance between the EPSP's input site and the proximally AHP conductance location [6] could potentially be the cause for the paradoxical phenomena.

Methods

The modeling of the piriform pyramidal neuron is executed by a NEURON simulator [7]. The cell is composed of a soma and a single unbranched dendrite [8]. The length and width of the dendrite are set at 1300 μm and 2 μm, while the length and width of the soma are at 10 μm and 10/π μm. The dendrite is reconstructed by 26 isopotential compartments of 50 μm length each. The passive parameters are the uniformly distributed membrane resistance (R_m) of 30000 Ω-cm^2 and the capacitance (C_m) of 1 μF/cm^2. Cytoplasmic resistance (R_i) is defined at 100 Ωcm. At the soma, the maximal voltage dependent channels are sodium conductance (g_{Na}) of 8571 pS/μm^2 and delayed rectifier potassium conductance (g_{DR}) of 628 pS/μm^2. At the dendrites, the maximal g_{Na} is 2.3 pS/μm^2 and the maximal potassium conductances contain M bb current conductance (g_m) of 0.014 pS/μm^2, g_{DR} of 5 pS/μm^2, maximal calcium dependent potassium conductance (g_{kCa}) of 2000 pS/μm^2, and maximal voltage dependent calcium conductance of (g_{Ca}) 0.06 pS/μm^2. The kinetics of these voltage dependent conductances that are described by the H&H equations and the calcium concentration including its incorporation into the model are based on a previous computer model by Mainen and Senjowsky [8]. The voltage-dependent and AHP generating conductances are located only in a 300 μm long proximal dendritic segment. The reversal potentials of the sodium, potassium and calcium currents are set at 50 mV, -90 mV and 140 mV, respectively. EPSP conductance is simulated by an α-function with a maximal conductance of 1 nS. The time to maximal conductance (τ) is 0.5 ms. The reversal potential of the EPSP is held at 0 mV.

As in the laboratory experiments, we induce a standard AHP by six action potentials, initiated during a somatic current injection of 100 ms. We measure AHP amplitudes relative to the resting potential of

-80 mV. In all the simulations, EPSP is introduced at the time of maximal AHP amplitude, *i.e.*, 50 ms after the termination of the 6th spike, and its depression is then compared to the control values. EPSP amplitude is always measured at the soma.

Results

Simulating the reduction of AHP amplitude

Under experimental conditions, the AHP-related EPSP reduction in the trained rats amounts to 16.5%, whereas the reduction in the naive and pseudo-trained rats is only 12.1% [2]. Paradoxically, the more effective inhibition of the EPSP in the trained rats is associated with a 19% decrease of AHP amplitude, an effect not observed in the control groups. The magnitude of the AHP conductance (g_{AHP}) yielding such an AHP amplitude depression is currently unknown. Three distinct alterations of the control parameters could potentially provide a similar decrease of the AHP amplitude: (1.) *"Conductance change:"* Decreasing g_{kCa} by 40% relative to the control levels, without any other changes in the set-up. (2.) *"Moving:"* Moving the location of the active conductance area distally from the soma, without altering its length. In order to reduce the AHP amplitude by 19%, the g_{kCa} has to be lowered too, but by only 15%. (3.) "*Shrinkage:*" Decreasing the length of the active conductance dendritic area from 300 μm to 100 μm, while increasing g_{kCa} by only 9%. The simulated action potentials and the resultant AHP levels turn out to be consistent with the experimental results (fig. 1).

EPSP reduction due to the AHP conductance (g_{AHP})

After obtaining a 19% reduction of AHP amplitude in each of the three models, we set the resting potential to the potassium's reversal potential (-90 mV, without any additional changes), in order to simulate the shunt effects of the g_{AHP} on the EPSP. We then initiate EPSP at the AHP maximal conductance, *i.e.*, 50 ms after the 6th spike. The isolated affected EPSP is obtained by subtracting the trace of the 6 spike alone from the trace of the 6 spike plus the EPSP. This isolated EPSP can be compared to the normal single EPSP (fig. 1) for evaluating the percent of inhibition (%inhibition=100($EPSP_{peak}$-isolated $EPSP_{peak}$)/$EPSP_{peak}$). We then systematically examine the effect of moving the EPSP input away (distal) from the soma in the three described models. As may be expected for a passive spread, somatic measured EPSP levels become smaller with distance. Surprisingly, however, the EPSP depression by the g_{AHP} turns out to be relatively more effective. The relation between the EPSP reduction and its site of initiation exhibits a sigmoidal function (fig. 2). In order to understand the cause of this depression, we also measure the EPSP at two other sites. First, we measure EPSP at the input site in the presence of g_{AHP}, but obtain a similar response with no decline (see curve with filled triangles in fig. 2). Second, we measure EPSP for each synaptic location at a compartment just distal to the active dendritic area (300 μm distal to the soma). The difference between the latter EPSP inhibition and the inhibition obtained at the soma amounts to 10-15% (fig. 2; compare filled rectangles curve with filled circles curve). The contribution of the active dendritic segment to the depression of the EPSP is, therefore, constant and independent of the synaptic input

location. However, increasing the distance between the active segment and the EPSP input location by additional passive segments significantly improves the EPSP depression by the g_{AHP}.

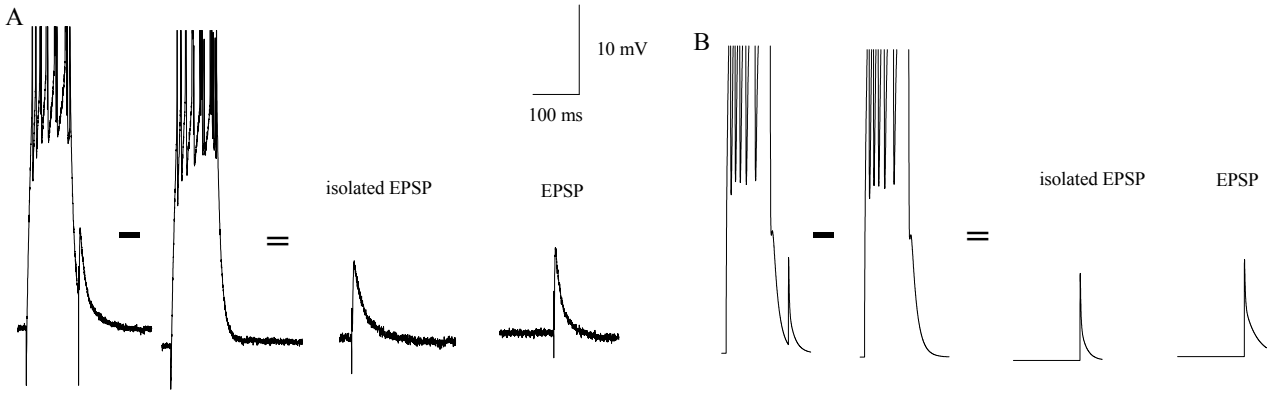

Fig. 1. Depression of EPSP during the maximal AHP conductance. EPSP was initiated 50 ms after the termination of the 6th spike. The resting potential was determined at -90 mV, the potassium reversal potential, in order to avoid hyperpolarization. An isolated EPSP was obtained experimentally (A; Saar, Grossman and Barkai, unpublished) and theoretically (B), after subtracting the response of the six spikes from the response, including these spikes and the EPSP. Subsequently, the isolated EPSP was compared with the control EPSP in order to determine its reduction.

The difference between the latter EPSP inhibition and the inhibition obtained at the soma amounts to 10-15% (fig. 2; compare filled rectangles curve with filled circles curve). The contribution of the active dendritic segment to the depression of the EPSP is, therefore, constant and independent of the synaptic input location. However, increasing the distance between the active segment and the EPSP input location by additional passive segments significantly improves the EPSP depression by the g_{AHP}. The above mentioned paradoxical phenomenon of increased EPSP depression, despite diminished AHP amplitude, can be explained by a "jump" from the control curve to one of the other curves that represent a 19% decreased AHP amplitude. Such a "jump" clearly entails a movement of EPSP input to a more distal point from the soma. According to the analyzed models, the process of learning could be as follows: under control conditions, AHP reduces EPSP amplitude by 12.1%. This fits a possible position of the EPSP input on the dendrite, 370 μm (y=12.1% of inhibition, x segment number = 2.4; distance from the soma is (2.4-1)·50 μm + 300 μm active dendrite) distally from the soma (fig. 2). In order to simulate a 16.5% decrease of EPSP by the AHP after training, when the AHP amplitude is reduced by 19%, the synaptic input has to "move" to either of the following possible locations on the dendrite:

Model 1: 690 μm (y=16.5, x= 8.8; (8.8-1)· 50+300 = 690).

Model 2: 710 μm (y=16.5, x= 9.2; (9.2-1)· 50+300 = 710).

Model 3: 555 μm (y=16.5, x= 7.9; (7.9-1)· 50+300 = 645).

The predicted EPSP location shift in Models 1, 2 and 3 are 320, 340 and 275 μm, respectively. We therefore suggest that, in all three models, the training associated changes result from a shift to distal location of the synaptic inputs.

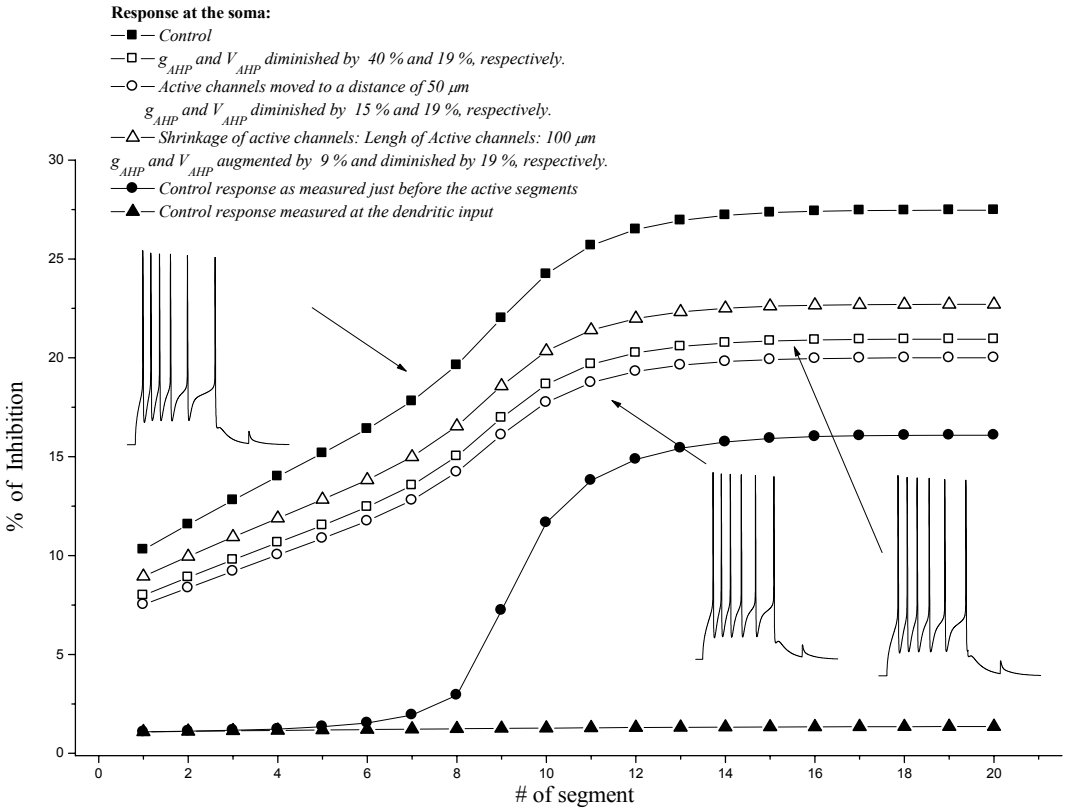

Fig. 2. A cellular model of learning, explaining the observation of enhanced EPSP inhibition by decreased AHP amplitude. The x-axis presents the 1000 μm long passive dendrite, divided to segments, each one with a length of 50 μm. In the control condition the soma is separated from this passive dendrite by a 300 μm long dendrite, containing active conductances. Segment "1" refers to the first passive segment next to the active dendrite. A 19% decrease of the AHP amplitude, as a result of learning, can be simulated by three models: (1.) Decrease of g_{KCa} by 40% (□, with no additional changes) (2.) reduction of the g_{KCa} by 15% and a distal movement of the active dendrite (○); (3.) and a shrinkage of the active dendrite and an enhancement of g_{Kca} (Δ). According to the experiments, after learning, g_{AHP} reduces EPSP by 16.1%. In order to enhance this inhibition after learning in all three models, the synaptic input locations have to move distally (275- 340 μm, see the text) from the soma. To simulate a g_{AHP} decrease, a parallel a "jump" from the control condition (■) to either one of the curves has to occur. The EPSP inhibition measured at the location of the synaptic input (▲) is equal along the dendrite. The difference between the EPSP inhibition recorded at the soma in the control condition (■) and the inhibition measured just before the active dendrite (●) in the same state is more or less constant, independent of the synaptic input location. This suggests that the length of the passive dendrite is the main cause for the distinct EPSP inhibition by the g_{AHP}.

Discussion and Conclusions

The main conjecture of the present simulation is that learning related changes in AHP and EPSP depression could be associated with a combination of reduction in the effective shunt of the AHP and a relative shift of the synaptic input distally from the soma. We tested three different models to explain the phenomena. While at this stage we cannot rule out any of the models to explain AHP reduction, Model 1 only involves a single parameter change (g_{KCa}) and is thus the simplest one. The expected

change, however, has to be large (40%). Models 2 and 3 involve additional parameters of shortening or shifting the AHP active membrane location, but the required shift in the synaptic input location in Model 3 is smaller than in Model 1. It is important to note that the olfactory learning process has previously been shown to involve long-term increase in spine density in the apical dendrites of piriform pyramidal cells [9]. However, no systematical comparison was carried out on the different parts of the basal and apical dendrites before and after the learning process. It is reasonable to assume that the change in spine density reflects general changes in functional synaptic input. Therefore we hypothesize that if the density of the distal synaptic input increases more than the proximal input, this consequently would lead to shift in the "center of gravity" (centroid) of the excitatory synaptic input [10].

The use of g_{KCa} to simulate modulation of AHP amplitude appears reasonable in light of earlier experimental evidence [11]. This is corroborated by BAPTA injection to the same cells [12], suggesting that this conductance is at least partially involved with the observed physiological changes.

Interestingly, our simulation analysis clearly indicates that the distance between the synaptic input and the g_{AHP} segment, which represents a passive dendrite segment, is crucial in determining the amount of EPSP depression recorded at the soma [13]. We previously reported similar results based on simulation of reconstructed α-motoneurons [14]. In that system, the proximally located inputs of reciprocal inhibition depress distally distributed Ia-EPSP inputs more efficiently than recurrent inhibition, whose synaptic inputs are co-localized with the excitatory inputs.

References

[1]. Saar, D., Y. Grossman, and E. Barkai, Reduced after-hyperpolarization in rat piriform cortex pyramidal neurons is associated with increased learning capability during operant conditioning. Eur J Neurosci, 1998. 10(4): p. 1518-23.

[2]. Saar, D., Y. Grossman, and E. Barkai, Reduced synaptic facilitation between pyramidal neurons in the piriform cortex after odor learning. J Neurosci, 1999. 19(19): p. 8616-22.

[3]. Saar, D., Y. Grossman, and E. Barkai, Learning-induced enhancement of postsynaptic potentials in pyramidal neurons. J Neurophysiol, 2002. 87(5): p. 2358-63.

[4]. Saar, D. and E. Barkai, Long-term modifications in intrinsic neuronal properties and rule learning in rats. Eur J Neurosci, 2003. 17(12): p. 2727-34.

[5]. Barkai, E. and D. Saar, Cellular correlates of olfactory learning in the rat piriform cortex. Rev Neurosci, 2001. 12(2): p. 111-20.

[6]. Sah, P. and J.M. Bekkers, Apical dendritic location of slow afterhyperpolarization current in hippocampal pyramidal neurons: implications for the integration of long-term potentiation. J Neurosci, 1996. 16(15): p . 4537-42.

[7]. Hines, M., A program for simulation of nerve equations with branching geometries. Int J Biomed Comput, 1989. 24(1): p. 55-68.

[8]. Mainen, Z.F. and T.J. Sejnowski, Influence of dendritic structure on firing pattern in model neocortical neurons. Nature, 1996. 382(6589): p. 363-6.

[9]. Knafo, S., et al., Olfactory learning is associated with increased spine density along apical dendrites of pyramidal neurons in the rat piriform cortex. Eur J Neurosci, 2001. 13(3): p. 633-8.

[10]. Agmon-Snir, H. and I. Segev, Signal delay and input synchronization in passive dendritic structures. J Neurophysiol, 1993. 70(5): p. 2066-85.

[11]. Sah, P. and J.D. Clements, Photolytic manipulation of [Ca2+]i reveals slow kinetics of potassium channels underlying the afterhyperpolarization in hippocampal pyramidal neurons. J Neurosci, 1999. 19(10): p. 3657-64.

[12]. Saar, D., Y. Grossman, and E. Barkai, *Long-lasting cholinergic modulation underlies rule learning in rats.* J Neurosci, 2001. 21(4): p. 1385-92.

[13]. Rall, W., *Distinguishing theoretical synaptic potentials computed for different soma-dendritic distributions of synaptic input.* J Neurophysiol, 1967. 30(5): p. 1138-68.

[14]. Gradwohl, G. and Y. Grossman, *Dendritic voltage dependent conductances increase the excitatory synaptic response and its postsynaptic inhibition in a reconstructed α-motoneuron: A computer model.* Neurocomputing, 2001. 38-40: p. 223-229.